

Determining the Relation Between the Count Number and X-Ray Energy Levels in Pyroelectric Materials

Submitted to the Graduate School of Natural and Applied Sciences
in partial fulfilment of the requirements for the degree of

Master of Science

in Biomedical Engineering

by

Saadet Sena Egeli

ORCID 0000-0002-7301-2446

November, 2021

This is to certify that we have read the thesis **Determining the Relation Between the Count Number and X-Ray Energy Levels in Pyroelectric Materials** submitted by **Saadet Sena Egeli**, and it has been judged to be successful, in scope and in quality, at the defense exam and accepted by our jury as a MASTER’S THESIS.

APPROVED BY:

Advisor: **Assoc. Prof. Dr. Yalçın İşler**
İzmir Kâtip Çelebi University

Committee Members:

Assist. Prof. Dr. Gökçenur Gökçe
 İzmir Kâtip Çelebi University

Assist. Prof. Dr. Mustafa Berkant Selek
 Ege University

Date of Defense: November 29, 2021

Declaration of Authorship

I, **Saadet Sena Egeli**, declare that this thesis titled **Determining the Relation Between the Count Number and X-Ray Energy Levels in Pyroelectric Materials** and the work presented in it are my own. I confirm that:

- This work was done wholly or mainly while in candidature for the Master's degree at this university.
- Where any part of this thesis has previously been submitted for a degree or any other qualification at this university or any other institution, this has been clearly stated.
- Where I have consulted the published work of others, this is always clearly attributed.
- Where I have quoted from the work of others, the source is always given. This thesis is entirely my own work, with the exception of such quotations.
- I have acknowledged all major sources of assistance.
- Where the thesis is based on work done by myself jointly with others, I have made clear exactly what was done by others and what I have contributed myself.

Signature:

Date:

29.11.2021

Determining the Relation Between the Count Number and X-Ray Energy Levels in Pyroelectric Materials

Abstract

Medical imaging is creating images of the interior body without any invasive operation. The discovery of x-rays establishes the foundation of medical imaging. Over time, new imaging modalities developed. Magnetic resonance imaging, positron emission tomography can be examples of these modalities. However, x-rays remained a cornerstone application. Like every imaging modality, x-rays also have disadvantageous features and need developments. New methods tried to generate x-rays to overcome generator-based issues. Pyroelectric crystal usage for x-ray generation is an example of novel x-ray generation methods. Pyroelectric crystals can create an electric field by thermally cycling. This electric field is used to obtain x-ray beams with a target material. X-ray generation with pyroelectricity has many advantages over the traditional method. Studies with pyroelectric crystals are still not clear for all the factors which affect x-ray yield. By understanding the generation process well, pyroelectric x-ray generators can be a part of medical imaging. Dental radiography devices especially can take advantage of small device designs. In this study, effect of count number of the crystal for pyroelectric x-ray generation was investigated with curve fitting methods to develop a miniature size, lightweight and low-cost dental radiography device.

Keywords: Pyroelectricity, X-ray, Curve Fitting.

Piroelektrik Malzemelerde Döngü Sayısı ile X Işını Enerji Seviyesi Arasındaki İlişkinin Belirlenmesi

ÖZ

Tıbbi görüntüleme, herhangi bir invaziv işlem olmaksızın vücudun içinin görüntülerini oluşturmaktır. X-ışınlarının keşfi, tıbbi görüntülemenin temelini oluşturur. Zamanla yeni görüntüleme yöntemleri de geliştirilmiştir. Manyetik rezonans görüntüleme, pozitron emisyon tomografisi bu yöntemlerin örnekleri olabilir. Bununla birlikte, x-ışınları bir temel uygulama olarak kalmıştır. Her görüntüleme yöntemi gibi, x-ışınları da dezavantajlara sahiptir ve geliştirmeye ihtiyaç duyar. Üreteç temelli sorunların üstesinden gelme amacıyla yeni x-ışını üretim metotları geliştirilmeye çalışıldı. X-ışını üretimi için piroelektrik kristal kullanımı, yeni x-ışını oluşturma yöntemlerine bir örnektir. Piroelektrik kristaller, termal döngü ile bir elektrik alanı oluşturabilir. Bu elektrik alanı, bir hedef malzeme ile x-ışınları elde etmek için kullanılır. Piroelektrik ile X-ışını üretimi, geleneksel yöntemle göre birçok avantaja sahiptir. Piroelektrik kristallerle yapılan çalışmalar, x-ışını verimini etkileyen tüm faktörler için hala net değildir. Üretim sürecini iyi anlayarak, piroelektrik x-ışını jeneratörleri tıbbi görüntülemenin bir parçası olabilir. Özellikle dental radyografi cihazları küçük cihaz tasarımlarından yararlanabilir. Bu çalışmada, minyatür boyutlu, hafif ve düşük maliyetli bir dental radyografi cihazı geliştirmek için piroelektrik x-ışını oluşturmada kristalin döngü sayısının etkisi eğri uydurma yöntemleri ile araştırılmıştır.

Anahtar Kelimeler: Piroelektrik, X-ışını, Eğri Uydurma.

Acknowledgment

I want to use this opportunity to express my gratitude to everyone who supported me throughout my education life, especially my dear family, and my venerable advisor, Yalçın İşler, who gave me enormous support and courage.

Table of Contents

Declaration of Authorship	ii
Abstract	iii
Öz	v
Acknowledgment	viii
List of Figures	xii
List of Tables	xiii
List of Abbreviations	xiv
List of Symbols	xv
1 Introduction	1
1.1 Medical Imaging	1
1.1.1 X-Ray Imaging	1
1.1.2 Computed Tomography	2
1.1.3 Nuclear Imaging	3
1.1.4 Magnetic Resonance Imaging	4
1.1.5 Ultrasound Imaging	4
1.2 Dental Imaging	5
1.2.1 Digital Radiography in Dental Imaging	6
1.3 X-Ray Production	7
1.3.1 X-ray Production Mechanism	7
1.3.2 X-ray Tube	8

1.4	Pyroelectricity	10
1.4.1	Physical Phenomena for Pyroelectricity	10
1.4.2	X-ray Generation with Pyroelectric Crystal	12
1.4.2.1	Environment Pressure	13
1.4.2.2	Heating Rate	13
1.4.2.3	Thickness of Crystal	13
1.4.2.4	Two Crystal Usage (Paired Crystal)	14
1.4.3	Scope of The Thesis	14
2	Materials and Methods	16
2.1	Data	16
2.2	Methods	16
2.2.1	Curve Fitting	16
2.2.1.1	Linear Regression	17
2.2.1.2	Exponential Curve Fitting	20
2.2.1.3	Fourier Series Curve Fitting	20
2.2.1.4	Gaussian Curve Fitting	20
2.2.1.5	Polynomial Curve Fitting	21
2.2.1.6	Power Series Curve Fitting	21
2.2.1.7	Rationals Curve Fitting	21
2.2.1.8	Smoothing Spline Curve Fitting	21
2.2.1.9	Sum of Sines	21
2.2.1.10	Weibul Distribution	22
2.2.1.11	Custom Equations	22
2.2.2	Statistical Package for the Social Sciences	22
2.2.2	MATLAB	23
3	Results and Discussion	24
3.2	Results	24

3.1 Discussion	31
4 Conclusion	33
References	34
Appendices	40
Appendix A Publications from the Thesis	41
Curriculum Vitae	42

List of Figures

Figure 1.1	Chest x-ray image	2
Figure 1.2	A section from computed tomography image	3
Figure 1.3	PET scan sample	3
Figure 1.4	MRI scan sample	4
Figure 1.5	Ultrasound image of foetus	5
Figure 1.6	Walkhoff's dental radiographs	6
Figure 1.7	An X-ray Tube Sample	8
Figure 1.8	The COOL-X x-ray generator from Amptek	9
Figure 1.9	First x-ray spectrum obtained from pyroelectric crystal	12
Figure 3.1	Fit graph of the example study 1	18
Figure 3.2	Fit graph of the example study 3	18
Figure 3.3	Fit graph of the example study 4	19
Figure 3.4	Exponential curve fitting for study 4	19
Figure 3.5	Polynomial curve fitting for study 2	19

List of Tables

Table 2.1	Pyroelectric crystal examples with their pyroelectric properties	10
Table 3.1	Statistical analysis results for linear regression models obtained from five distinct studies in the literature.....	23
Table 3.2	Goodness of fit results for study 1	26
Table 3.3	Goodness of fit results for study 2	26
Table 3.4	Goodness of fit results for study 3	27
Table 3.5	Goodness of fit results for study 4	27
Table 3.6	Goodness of fit results for study 5	28
Table 3.7	Curve fitting equations for studies	29

List of Abbreviations

2D	Two Dimensional
3D	Three Dimensional
CBCT	Cone Beam Computed Tomography
CT	Computed Tomography
GUI	Graphical User Interface
keV	Kilo electronvolts
kHz	Kilohertz
kVp	Kilovolt-peak
MHz	Megahertz
MRI	Magnetic Resonance Imaging
PET	Positron Emission Tomography
RF	Radio Frequency
SSR	Sum of the Squares related to the Regression
SST	Sum of the Squares Total
SPECT	Single Photon Emission Computed Tomography
SPSS	Statistical Package for the Social Sciences
TACT	Tuned Aperture Computed Tomography
US	Ultrasound

List of Symbols

A	Surface Area
C	Capacitance
Δ	Change
ε	Dielectric permittivity
γ	Gamma
P_s	Spontaneous polarization
ρ	Pyroelectric coefficient
Q	Surface charge
V	Electric potential

Chapter 1

Introduction

1.1 Medical Imaging

Medical imaging is the summation of techniques used to create images of the internal body by aiming to diagnose, treat or intervene. Medical imaging techniques help professionals by representing internal structures in the body that cannot be seen by the naked eye without invasion. These non-invasive techniques affect healthcare effectiveness positively and have a profound effect on medicine. Medical imaging history starts with the discovery of X-rays, a type of radiation that can penetrate the body. In the beginning, X-rays were used to create images of the inter-body, looking ahead today, many other imaging modalities developed after X-ray imaging. Today, Computed Tomography, Nuclear Imaging, Magnetic Resonance Imaging and Ultrasound Imaging are examples of medical imaging modalities.

1.1.1 X-Ray Imaging

In 1895 physicist Wilhelm Conrad Rontgen discovered a new ray type, the discovery started a new era [1]. Rontgen called these rays X-rays; by their help, he took the first radiograph of a human by imaging his wife's hand bones with these rays [1]. After a short time of discovery, X-rays started to use in medicine and dentistry [2,3]. X-rays lose their energy when they transmit through matter; the amount of attenuation depends on the matter's characteristics. Radiographic images are obtained by basing this attenuation, X-rays send to the body and then attenuated

beams get captured with film or digital detectors. Inside the body different tissue characteristics also lead to distinct representation in the image, dark images from soft tissues and whiter images from hard tissues like bones. By considering these, to image the body accurately, every part needs to get imaged by X-rays in different energy levels. Mammography, displaying the breasts with X-rays, requires 25-35 kilovolt-peak (kVp) X-rays. Fluoroscopy, real-time imaging of internal organs with X-rays, requires 60-120 kVp and general purposed radiographs (like hand, mandible, knee, chest) 54-120 kVp used (see Figure 1.1) [4,5].



Figure 1.1: Chest x-ray image [6]

1.1.2 Computed Tomography

X-ray imaging evolved in time to meet the needs in the medical imaging field yet, images obtained from this method have two-dimension. Two-dimensional (2D) images aid to detect diseases and abnormalities although, they are insufficient since the structures in the body are three-dimensional (3D). To overcome this problem, in 1972 Hounsfield and Cormack invented a new X-ray device integrated with the computer to create 3D images of the structures in the body [7]. In this modality cross-sectional images, which are called projections, are obtained by scanning the body in multiple directions gathered by different back-projection methods to create a 3D image. Computed Tomography device has five generations to image various parts of the body or varies by movement type, but all these generations use X-rays and have a wide range of application areas (see Figure 1.2) [8].



Figure 1.2: A section from computed tomography image [6]

1.1.3 Nuclear Imaging

Nuclear imaging or nuclear medicine uses radioactive substances to image the patient's body or treat the patient. Radioactive substances may inject into veins, maybe breathed, or ingested by the patient [9]. These radioactive substances, also called radiopharmaceuticals, emit gamma rays (γ -rays) while the body is functioning. These rays are another type of radiation. To form an image, captured by a gamma camera (anger camera) (see Figure 1.3) [11]. Gamma camera helps to measure the concentration of the radioactive substances, also functional information about the body obtained. Scintigraphy, Single-photon emission tomography and Positron emission tomography are types of nuclear imaging [5,10,13].

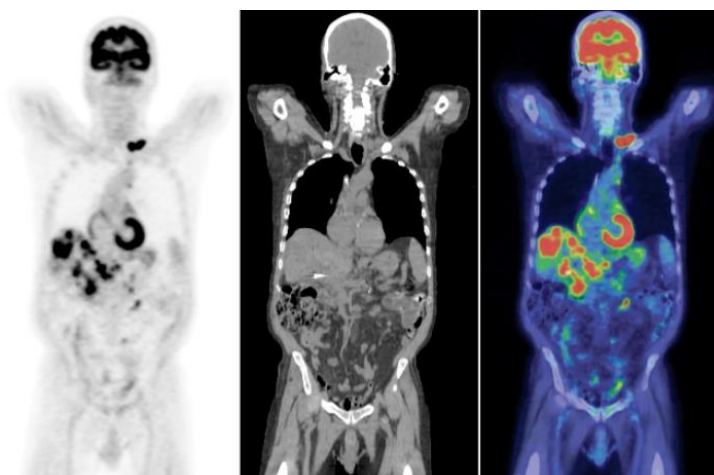


Figure 1.3: PET scan sample [12]

1.1.4 Magnetic Resonance Imaging

Magnetic Resonance Imaging (MRI) is another imaging modality frequently used in medicine. MRI is based on the nuclear magnetic resonance phenomenon; this method does not use ionizing radiation. Atoms possess nuclear magnetic moment; in standard conditions, this moment is randomly oriented. When an external magnetic field is applied, this orientation changes into parallel or anti-parallel with this magnetic field. Next, a second magnetic field is applied and results in radio frequency (RF) which produces a required signal for imaging. This RF signal is detected by RF coils and sent to the computer to form the image (see Figure 1.4) [10]. MRI has a high 3D imaging capacity and helps to diagnose tumours, spinal injuries or diseases in the brain and heart [12,13].



Figure 1.4: MRI scan sample [10]

1.1.5 Ultrasound Imaging

Ultrasound is defined as the sound waves which have frequencies above 20 kilohertz (kHz) [15]. In medicine, ultrasound waves are used as a medical imaging technique due to the acoustic properties of tissues. In the generation of ultrasound waves, transducer elements are used, this element is generally a piezoelectric crystal. After the generation of the wave, it is transmitted through the body part that needs to get imaged. Waves particularly reflect between tissues; these reflections give

information about the depth of tissue and help to create the image. The reflections were detected by the piezoelectric material in the ultrasound probe and converted to electrical signals and images (see Figure 1.5). Every tissue has different acoustic properties and ultrasound imaging takes advantage of these differences to image tissues distinctively [12,16,17].

Ultrasound imaging is frequently used because of its low-cost and non-ionizing nature; in these applications, 2-15 megahertz (MHz) waves are preferred [15]. This imaging modality helps to image soft tissues. The application is operator dependent [5].



Figure 1.5: Ultrasound image of foetus [16]

1.2 Dental Imaging

The history of dental imaging starts just after the discovery of X-rays. In 1896, Dr Otto Walkhoff used X-rays to image his mouth (see Figure 1.6) [18]. From this first application, x-ray usage in dentistry remained a cornerstone. With the help of x-rays, primarily, the tooth decays become more observable. Also, diagnoses of bone losses and abnormalities in dental structure get easy for professionals. Today, digital radiography and computed tomography are the most used imaging modalities in dental imaging.

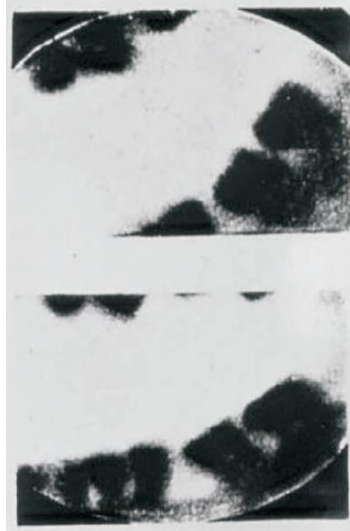


Figure 1.6: Walkhoff's dental radiographs [18]

1.2.1 Digital Radiography in Dental Imaging

Dental imaging practice on plain radiography with two methods; intraoral radiography and extra-oral radiography. For intraoral radiography, x-ray receptors are placed into the mouth to image the region. Intraoral examinations have three distinct groups which use different imaging receptors and techniques. The periapical radiography is for imaging the entire tooth. Interproximal radiography is to image tooth crown and occlusal radiography for imaging of jawbones [19].

The other method is extra-oral radiography. In this method, the receptor is placed outside of the mouth. By changing the head position, receptor placement and exposure factor, images can be useful for different purposes. Extra-oral radiographs' application examples are lesion and disease detection, examining sizeable areas of the jaw and growth evaluation [19].

The need for three-dimensional imaging of the structures is also valid for dental imaging applications. For this reason, the computed tomography method is extensively used in dentistry. CT application in dentistry covers implant displacement, the definition of anatomic structures, temporomandibular joint, pathology and orthodontic evaluations [19]. Tuned Aperture Computed Tomography (TACT), Micro Computed Tomography (Micro-CT) and Cone Beam Computed

Tomography (CBCT) are types of dental CT applications [20]. From these three, CBCT applications have revolutionary effects for this field. CBCT scans help to locate tumours, bone lesions, accurate identifications of root canals and are useful for implant dentistry applications [19].

Together with mentioned applications, other imaging modalities are also studying to advance dental imaging like; Nuclear imaging, Magnetic resonance imaging, and Ultrasound imaging [20]. Nuclear imaging methods are appropriate for calcification problems and periodontium diseases [20]. Although magnetic resonance imaging is better for imaging soft tissues, there are its applications in dentistry. Since x-ray based methods are not appropriate for imaging soft tissues, the salivary glands and other soft tissues may be imaged with magnetic resonance imaging [20]. Ultrasound in dentistry provides both hard tissue and soft tissue imaging. Dental fractures and soft tissue lesions are examples of ultrasound application in dentistry [21].

1.3 X-ray Production

1.3.1 X-ray Production Mechanism

As a fundamental mechanism, X-ray production can be described as the bombardment of the target material with high-energetic electrons. When we look into details, there are two different mechanisms of X-ray production however, both of these mechanisms require high energetic electrons and target material. The first type is Bremsstrahlung X-ray, a German word that means “braking radiation”. Bremsstrahlung X-ray is the result of the deceleration of electrons. The accelerated electrons are sent to the target and if these electrons pass near the target atoms’ nucleus, an attraction between these particles results in deceleration of electrons and the energy lost by electrons produces heat and X-rays. Mainly the X-rays produced in this method, and it observed that if the distance between electron and nucleus decreases the energy of X-ray increases [13].

The other type is the Characteristic X-ray. These rays resulted from the interaction between accelerated electrons and the orbital electron of the target material. When an accelerated electron interacts with the target, this causes excitation in the electron

and a vacancy in the orbital. The vacancy is filled with another electron from a higher orbit and during the falling of this electron excessive energy is emitted as an X-ray [15]. This type of X-ray is called a characteristic X-ray since the energy difference of different orbits varies for every atom the energy of emitted X-ray changes [22].

1.3.1 X-ray Tube

Wilhelm Roentgen discovered the X-rays while he was experimenting with Crook tubes for cathode rays [23]. Therefore, the tubes used to generate X-rays are like the Crook tubes. X-ray tubes are glass, vacuum tubes and use electrical energy to generate the rays (see Figure 1.7). An X-ray tube has different parts; cathode, anode, tube housing and shielding material [24]. The cathode is the source of electrons that will be accelerated for bombarding the target material. Cathode material was chosen as a metal with a high melting point, generally, tungsten filaments are used because its melting point is 3410°C. However, tungsten is also used since it has a low tendency to vaporise and good conductor [16]. The filament placed in a focusing cup is generally made up of molybdenum or nickel [14]. The anode is the target material for X-ray generation, made up of tungsten or molybdenum again because of physical characteristics. Most of the energy of accelerated electrons is converted into heat in the anode, as described before while generating X-ray heat energy is also created. Because of this, an important criterion for choosing anode material is heat capacity. To avoid excessive heating of the anode, rotating anodes are developed, and the tube is surrounded by oil to insulate this heat. The tube is a vacuum because the interaction of cathode and anode with gas may result in damage for X-ray generation, Pyrex glass is used for tube material [13]. Since generated X-ray is not focused on one direction, the tube must be shielded to avoid radiation dissemination to other directions, this will protect the patient and the professionals. To shielding, lead is generally preferred [25].



Figure 1.7: An x-ray tube sample

Early in the history of X-rays, Siemens & Halske received the first patent of X-ray tubes [26,27]. After that other X-ray tubes were designed to solve problems like heat loading, intensity, and penetration. These basic components of the X-ray tube described above, formed over time. In the present day, there are still problems with X-ray emission in all ways, incoherence nature of X-rays, tube lifetime, tube costs and electrical costs due to energy requirement [28]. To advance the X-ray technology for efficient and effective X-rays, new generation sources are being developed. Example of these sources is Synchrotron radiation, free-electron lasers, laser wakefield X-ray sources, Carbon nanotube-based X-ray and Pyroelectricity for X-ray production [29,30].

The alternative methods for x-ray generation did not replace whole traditional x-ray generators. Nonetheless, these alternatives started to take place in the market. As an example, the COOL-X x-ray generator from Amptek company is commercially available (see Figure 1.8). This generator uses pyroelectric crystals for x-ray generation [31]. When its specification is examined, battery options, low energy consumption, and miniature size draw attention. The company explains its applications like portable x-ray instrumentation, teaching laboratories, instrument calibration, research and radiography [31]. Isler et al. [32] investigated this generator for suitability in medical imaging applications. In that study, the conventional x-ray tube and pyroelectric x-ray generator were compared. In conclusion, due to the advantages of the pyroelectric generator, it is stated as medical imaging applications also may be possible [32].

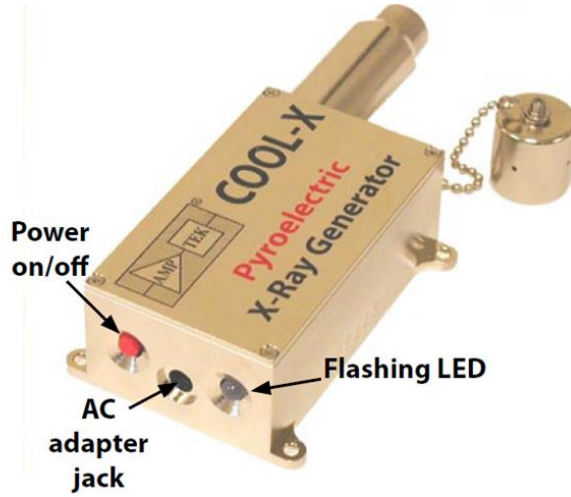


Figure 1.8: The COOL-X x-ray generator from Amptek [31]

1.4 Pyroelectricity

Pyroelectric materials are a type of piezoelectric materials and generate an electric field when the material temperature changed [33]. Pyroelectric materials known since ancient times however, applications of it increased in the 1960s [34].

1.4.1 Physical Phenomena for Pyroelectricity

Pyroelectric crystals normally have a polarization, dipole moment per unit volume, called spontaneous polarization (P_s) [33]. This polarization will never equal zero for pyroelectric materials and differentiating the temperature leads to a change in this polarization [35]. The pyroelectric coefficient (ρ) of the material is another factor while spontaneous polarization occurs. The relationship between these parameters can be summarized as in Equation 1.1.

$$P_s = \rho \Delta T \quad (1.1)$$

For this polarization to occur also a condition must be met, the Curie temperature of the material must not be exceeded. Curie temperature or curie point is the temperature to lose ferroelectric or piezoelectric properties of the material [36]. In Table 1.1, curie points and pyroelectric coefficients of some crystals are given.

Table 1.1: Pyroelectric crystal examples with their pyroelectric properties [34-36]

Crystal	Curie Point (°K)	Pyroelectric Coefficient($\mu\text{C}/\text{m}^2\text{°K}$)
BaTiO ₃ (Barium titanate)	396.15	100
CdS (Cadmium sulfide)	11.91-20.22	4.0
CsNO ₃ (Caesium nitrate)	472	4.3
LiNbO ₃ (Lithium niobate)	1480	4.0
LiTaO ₃ (Lithium tantalate)	813-973	190
NaKC ₄ H ₄ O ₃ H ₂ O	322	250
(ND ₂ CH ₂ COOD) ₃ D ₂ SO ₄ (Deuterated TGS, DTGS)	3366	270

Electron production from pyroelectric material is the basic principle for X-ray production. To emit electrons from a crystal, the electric potential (V) created is an important factor. An electric potential can be written in the form of surface charge (Q) and capacitance (C) (Equation 1.2). Surface charge affected by spontaneous polarization change ΔP_s and the surface area (A) Equation (1.3).

$$V = Q/C \quad (1.2)$$

$$Q = \Delta P_s A \quad (1.3)$$

Studies for using pyroelectric materials to generate electron beams started with studies by Rosenblum, Braunlich and Carrico in 1974 [41]. In their study, LiNbO₃ was used and after heating this crystal from room temperature to 100°C at a rate of 20°C per minute and crystal emitted electrons at a current 10^{-10} - 10^{-9} amperes (see Figure 1.9) [41]. In 2002, Brownridge & Shatrof also studied with LiNbO₃, for this study crystal was heated up to 160°C and obtained electron beams with ~170 kilo electron volt (keV) [42]. Electron beams occur when the electric field is large enough

to eject these electrons from the surface of the crystal. Electron beams are created both on the heating and cooling phases of the crystal. The emission surface depends on the phase, on the heating phase +z surface emits electrons and on the cooling phase -z surface emits electrons [43]. In the study of Brownridge & Shatrof also the effect of environmental pressure on to electric field was explained. It is explained as reduced pressure makes the electric field last longer [44].

1.4.2 X-ray Generation with Pyroelectric Crystal

Electron beam generation experiments lead to new experiments with pyroelectric crystals. In 1992, Brownridge published an article about his study with pyroelectric crystals to generate X-rays. For this study, CsNO_3 crystal thermally induced between 77°K to 300°K in a vacuum environment at 5×10^{-5} Torr pressure, resulting in electron beam bombarded gold (Au) target foil and X-rays generated [44]. These X-rays resulted from vacancies produced in L shell in target atoms' and the spectrum is given in Figure 1.9.

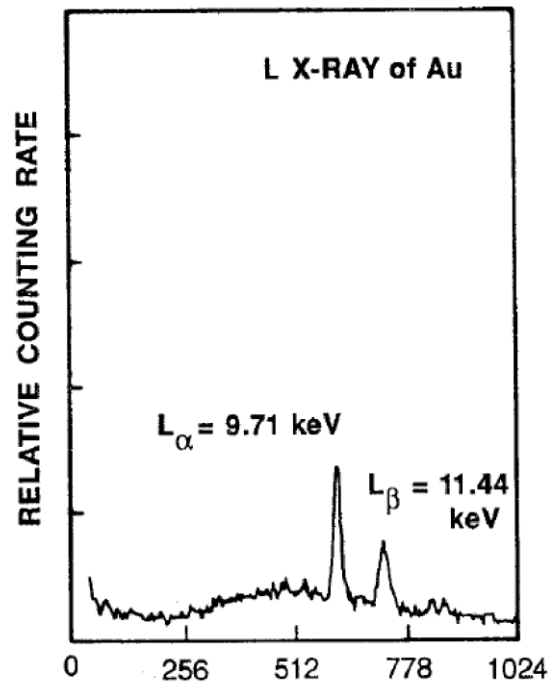


Figure 1.9: First x-ray spectrum obtained from pyroelectric crystal [41]

Investigations for X-ray production with pyroelectricity continued after this study. Scientists started to use different pyroelectric crystals like LiNbO_3 , LiTaO_3 and studied the effects of different parameters for more efficient X-ray production. For

example, Danon reported X-ray emission increases in the cooling phase of the crystal and decreases when cooling slows down [37]. Some other factors and their effects are explained briefly in the next parts.

1.4.2.1 Environment Pressure

To prevent damage of air X-rays generated in a vacuum environment whether classical X-ray generation methods or pyroelectric based methods. Example studies which are given before done in low pressures (10^{-3} - 10^{-6} Torr). Low pressure was chosen since it is known as X-ray intensity and pressure is inversely related. There are also examples in the pyroelectric generation which verifies this statement. A study with LiTaO_3 at 6×10^{-4} - 3×10^{-2} showed when ambient pressure decreased, X-ray intensity and endpoint energy increased [45].

1.4.2.2 Heating Rate

To create the electron beam, the pyroelectric crystal needs to be heated and cooled to change the electric field. The time of this thermal cycle also affects the yield of X-ray production. Geuther & Danon found that too fast or too slow thermally cycling the crystal reduces X-ray yield [47]. Another result of this study was, according to their observations, the optimum heating rate is about half the rate at which the crystal could no longer react to the entire thermal cycle [46].

1.4.2.3 Thickness of Crystal

In 2016, Hanamoto et al. investigated the effect of the low pressures on X-ray generation processes [47]. In this study, also the effect of the crystal thickness on potential is described by assuming the crystal as a parallel-plate capacitor. According to this assumption, potential can be calculated as:

$$V = \Delta T \cdot d \cdot \rho / \epsilon_0 + \epsilon_r \quad (1.4)$$

Where ΔT is the temperature change, ρ is the pyroelectric coefficient of the crystal, d is the thickness of the crystal and ϵ_0 and ϵ_r are dielectric permittivity of vacuum and

crystal respectively. From the equation, the thickness of the crystal and the potential relationship can be seen as directly proportional. Also, the other studies in the literature prove this relationship. Higher potential on crystal surface results in higher energetic electron beams and X-rays as stated before. Geuther & Danon demonstrated this relationship in their study with LiTaO_3 with 1mm, 2mm, 4mm and 10mm thickness and they concluded as the relationship between crystal thickness and X-ray energy yield is almost linear [46]. However, in the study of Danon, thicknesses greater than 10 mm were tested and showed that this linear relationship breaks down at 10 mm, for example, 20 mm thickness crystal results even less than the 10 mm crystal [37].

1.4.2.4 Two Crystal Usage (Paired Crystal)

Increasing the yield of pyroelectric X-ray generation is affected by different factors by basing the properties of pyroelectric crystals. There is another factor that may affect this yield by basing the superposition principle. In this principle, pyroelectric crystals can be placed together to enhance acceleration and thus the x-ray energy. By using two crystals as one cathode and one anode, the electron and x-ray energy may be doubled [37]. In the study of Geuther & Danon, one crystal resulted in 21 keV energetic X-ray and the addition of a second crystal increased this energy to 45 keV [46].

1.4.2 Scope of The Thesis

Medical imaging became essential for diagnosing and treatment for many medical conditions. Digital radiography devices are still a crucial part of medical imaging. These radiography devices have considerable advantages; however, they have also drawbacks. The costly and massive dimension devices and their energy consumption are examples of these drawbacks. Additionally, the energy need for x-ray generation is also high. To overcome these problems, new methods developing like pyroelectric crystal-based x-ray generation. Pyroelectric crystal x-ray generation does not require high voltages like the traditional method. Also, generator dimensions are minor. Pyroelectric x-ray generation depends on several factors. However, the net effects of these parameters on x-ray generation are not well known. This thesis aimed to

investigate one of these parameters, the relationship between crystal's heating and the cooling cycle number and x-ray energy; to develop a miniature size, lightweight and low-cost dental radiography device.

Chapter 2

Materials and Methods

2.1 Data

For this work, five graphs from four studies of pyroelectric x-ray generation were selected. In the literature, there are also other studies about pyroelectric x-ray generation. However, selected studies include detailed information about crystal properties, environment pressure and more clear graphs to obtain necessary data. Three studies use LiTaO_3 crystal; one study uses LiNbO_3 crystal to generate x-ray [35,43,47,48]. Two graphs of these studies are in the range of 0-200 count number while the other three have 0- 10^5 . For the x-ray energy range, the maximum obtained energy is 250 keV.

2.2 Methods

2.2.1 Curve Fitting

Curve fitting is a crucial mathematical modelling method used generally to understand system performance. A data set was obtained with experimental methods used for curve fitting. As a basic definition, curve fitting is the process for convergence of a given data set into a closed function [49]. Curve fitting plays a role in simulations, statistical assumptions and model predictions. Curve fitting aims to choose a function to minimize the error of data points in the cluster [49]. Curve fitting not only fits unorganized data into various models, but also performs a variety

of tasks such as reducing noise, finding mathematical relationships between variables, and evaluating attributes between data samples. [54] Some different approaches for curve fitting are Least-squares, median least squares, genetic algorithms and simulate annealing [49]. Regression and interpolation are also widely used for curve fitting in problem-solving. The least-squares method is used in linear regression to fit a curve for a given dataset. In this method, a line equation minimizes the sum of the squares of the errors for line approximation.

2.2.1.1 Linear Regression

Regression analysis is one of the most used analysis methods in statistics. This analysis method investigates the relationship between variables to estimate the value of one variable based on other variables or variables. Regression can be accomplished in two methods: simple linear regression and multiple linear regression. The difference between this method is the number of variables. Multiple linear regression predicts the one value based on multiple variables which makes it a type of multivariable analysis [50]. Simple linear regression uses one variable, independent (y), to calculate the other variable, dependent (x). The output of the linear regression is given in Equation (2.1).

$$y = \alpha_1 x + \alpha_0 \quad (2.1)$$

In this output, α_0 and α_1 are coefficients of regression. For statistical analysis to be done, different assumptions were made for different analysis methods. To do a simple linear regression analysis, four assumptions were done. Normality, homoscedasticity, linearity, and independence [50].

With the least-square method, Equation (2.1) is calculated in these steps given below.

$$y = \alpha_0 + \alpha_1 x + \varepsilon \quad (2.2)$$

$$\varepsilon = y_{real} + y_{approximate} = y - (\alpha_0 + \alpha_1 x) \quad (2.3)$$

$$S_r = \sum_{i=0}^n \varepsilon_i^2 y_i = \sum_{i=1}^n (y - \alpha_0 + \alpha_1 x)^2 \quad (2.4)$$

In Equation S_r is the sum of the squares of errors, α_1 is the slope of the line, α_0 intersection point, ε is the error. The α_1 and α_0 values to minimize the sum of squares find by equating zero the derivatives of these values Equation (2.6).

$$(n)\alpha_0 = (\sum x_i)\alpha_1 = \sum y_i \quad (2.5)$$

$$(\sum x_i)\alpha_1 = (\sum x_i^2)\alpha_1 = \sum x_i y_i \quad (2.6)$$

After these steps, values can express as in Equations (2.7 and 2.8).

$$\alpha_0 = y - \alpha_1 x = \frac{\sum y_i}{n} - \alpha_1 \frac{\sum x_i}{n} \quad (2.7)$$

$$\alpha_1 = \frac{n \sum x_i y_i - \sum x_i \sum y_i}{n \sum x_i^2 - (\sum x_i)^2} \quad (2.8)$$

Correlation coefficient (r) of this model is calculated as in Equation (2.9).

$$R = \frac{n \sum x_i y_i - \sum x_i \sum y_i}{\sqrt{n \sum x_i^2 - (\sum x_i)^2} \sqrt{n \sum y_i^2 - (\sum y_i)^2}} \quad (2.9)$$

Linear regression also outputs other values about the model to show the efficiency of the analyse. One of these variables is the “p-value”. The p-value indicates the extent to which the data fit the model predicted by the test hypothesis and all other assumptions used in the test [51]. H_0 hypothesis assumes that there is no difference between two groups for a specific variable. For the p-value, another definition is the probability of rejecting the H_0 hypothesis [51]. The p-value needs to be compared to a level to determine the statistical significance. The standard for this decision is generally stated as 0.05, as proposed earlier [51]. The p-value smaller than 0.05 means there is a statistical difference between the investigated variables where a p-value greater than 0.05 shows there is no statistical difference.

The Pearson correlation coefficient “R” and coefficient determination “R-square” are also the outputs. R-value is a measure of the degree of linear correlation between two variables. R-value has range between -1 and +1 where $r=0$ indicates no correlation [51,53]. R-square informs about the amount of variation in the dependent variable (y) due to the independent variable (x) [48]. It is calculated by using “Sum of squares related to the regression (SSR)” and “Sum of squares of total (SST)” [54]. SSE is calculated from the sum of the squares of the observed value and predicted value. SST is calculated from the sum of the squares of the observed value and mean value [54].

$$R^2 = 1 - \frac{SSR}{SST} \quad (2.10)$$

R-square is also between -1 and +1; bigger values imply a better fit for the model [56]. Adjusted R-square value is proposed to reduce the bias in R-square value [55]. This value is computed by using Equation 2.11 where “n” is the number of observations and the “p” the number of parameters in the calculated model [55].

$$R_a^2 = \frac{SSR/p}{SST/(n-1)} \quad (2.11)$$

2.2.1.2 Exponential Curve Fitting

Exponentials are frequently used for expressions that show a rate of change. By using this method Equation (2.12) is obtained.

$$y = \alpha e^{bx} \quad (2.12)$$

The coefficients of the “e” give the information for if there is decay (negative coefficient) or is a growth (positive coefficient) [57].

2.2.1.3 Fourier Series Curve Fitting

The Fourier Series represents a periodic signal utilizing the sum of sine and cosine functions.

General Equation for the Fourier Series model:

$$f(x) = a_0 + \sum_{i=1}^n a_i \cos(xw) + \sum_{i=1}^n b_i \sin(xw) \quad (2.13)$$

where a_0 models any DC offset in the signal and is associated with the $i = 0$ cosine term, w is the fundamental frequency of the signal, n is the number of terms (harmonics) in the series, and $1 \leq n \leq 8$ [57].

2.2.1.4 Gaussian Curve Fitting

To fit the peaks, the Gaussian model was used. The equation for this model is given as:

$$f(x) = \sum_{i=0}^n a_i e^{-\left(\frac{x-b_i}{c_i}\right)^2} \quad (2.14)$$

2.2.1.5 Polynomial Curve Fitting

Polynomial curve fitting uses the sine function to fit the best equation for the data points.

$$f(x) = p_1x + p_2 \quad (2.15)$$

2.2.1.6 Power Series Curve Fitting

Power series can be defined as in Equation 2.6 and have a wide range of applications

$$f(x) = ax^b \quad (2.16)$$

2.2.1.7 Rationals Curve Fitting

These models defined as ratios of polynomials also have flexibility with a complex data structure [57].

$$f(x) = \frac{p_1}{(x + q_1)} \quad (2.17)$$

2.2.1.8 Smoothing Spline Curve Fitting

The smoothing spline method can be preferred to fit the noisy data. Smoothing parameter p and the specified weight w_i are used to constructing the smoothing plane s . For the equation of this curve-fitting model, piecewise polynomials are computed from p .

2.2.1.9 Sum of Sines

To fit the periodic functions, the sum of the sine model can be preferred.

$$f(x) = \sum_{i=1}^n a_i \sin(b_i x + c_i) \quad (2.18)$$

where a is the amplitude, b is the frequency, and c is the phase constant for each sine wave term. n is the number of terms in the series and $1 \leq n \leq 8$.

2.2.1.10 Weibull Distribution

The Weibull distribution is used in reliability data analysis.

$$y = \alpha b x^{b-1} e^{-\alpha x^b} \quad (2.19)$$

In this equation, α is the scale parameter and b is the shape parameter.

2.2.1.11 Custom Equations

When the other models do not give the desired output, custom equations can be created.

2.2.2 Statistical Package for the Social Sciences

Statistical Package for the Social Sciences (SPSS) is a widely used software package released first in 1968. This package of programs is useful for data analysing, manipulating, and presenting [58]. Although its name includes social sciences, SPSS has applications in different areas like business, health research, education, and every field in which statistical analysis is necessary [59].

In this study, SPSS used to investigate the relationship between the count number of pyroelectric crystals and the x-ray energy. For this aim, simple linear regression analysis was applied.

First, data obtained from graphs were entered into the SPSS. After data entrance to the system, to perform linear regression; from the "Analyze" menu, the "Regression" tab selection and "Linear..." tab are selected. These steps open a dialogue box to choose variables; the independent variable is determined as count number (x); the

dependent variable is the x-ray energy (y). The outputs of the analysis open in a new window.

For a regression line in SPSS, the "Graph" menu is selected; in this menu, the "Legacy Dialogs" tab opened and the "Scatter/Dot..." option selected. For this study, the "Simple Scatter" option was selected. To add the regression line, from the output window the "Elements" menu in the output window and "Fit line at total" and "Linear" options were selected.

2.2.3 MATLAB

MATLAB® is a tool used for programming to analyse and design systems by computing and visualizing the data. The MATLAB language is based on the matrix to be compatible with the natural expressions of computational mathematics [58]. MATLAB® has a wide range of applications in different study fields like deep learning, image processing, computational biology; used by many engineers and scientists [60].

In this study, MATLAB® R2021B (Academic License supported by Izmir Katip Celebi University) was used to fit a curve for the investigation of the relationship between the count number of pyroelectric crystals and the x-ray energy. For that purpose, the Curve Fitting Toolbox of MATLAB was used. The Curve Fitting Toolbox is a collection of graphical user interfaces (GUIs) and M-file functions built on MATLAB® [60].

First, the obtained data from a study entered as array y (x-ray energy) and x (count number) arrays into a new .m file. For the next command line, "cftool" wrote to open the Curve Fitting Toolbox. After opening the toolbox, data were selected from the arrays as "Y Data" and "X Data", later different model types were selected for every five studies. The graphs of curve fittings, equation coefficients and goodness of fit values were obtained.

Chapter 3

Results and Discussion

3.1 Results

The linear regression model between x-ray energy values and count was calculated for five different studies from the literature. For each graph from studies, a minimum of thirty data points was obtained to create the models. The model summaries for each paper are shown in Table 3.1. In this summary, R-value, R^2 -value, and p-value are given.

Table 3.1: Statistical analysis results for linear regression models obtained from five distinct studies in the literature

	Material	R	R^2	Sig.(p)
Study 1 [36]	LiTaO ₃	0.96	0.91	0.00
Study 2 [36]	LiTaO ₃	0.31	0.01	0.11
Study 3 [42]	LiTaO ₃	0.83	0.69	0.00
Study 4 [28]	LiTaO ₃	0.92	0.85	0.00
Study 5 [42]	LiNbO ₃	0.12	0.01	0.70

The linear regression gives coefficients for the equation, this equation for each model shown in Equation 3.1, 3.2, 3.3, 3.4, and 3.5.

$$Energy_1 = -0.02 \text{ Count} + 233 \quad (3.1)$$

$$Energy_2 = 0.62 \text{ Count} + 83.72 \quad (3.2)$$

$$Energy_3 = -2.34 \text{ Count} + 22.99 \quad (3.3)$$

$$Energy_4 = -0.02 \text{ Count} + 193 \quad (3.4)$$

$$Energy_5 = -0.04 \text{ Count} + 34.69 \quad (3.5)$$

The fit graphs for the models with a p-value smaller than 0.05 are given in Figure 3.1, 3.2. and 3.3. The given graphs show how much the linear regression equation fits into the given data points (see Figure 3.1, 3.2 and 3.3).

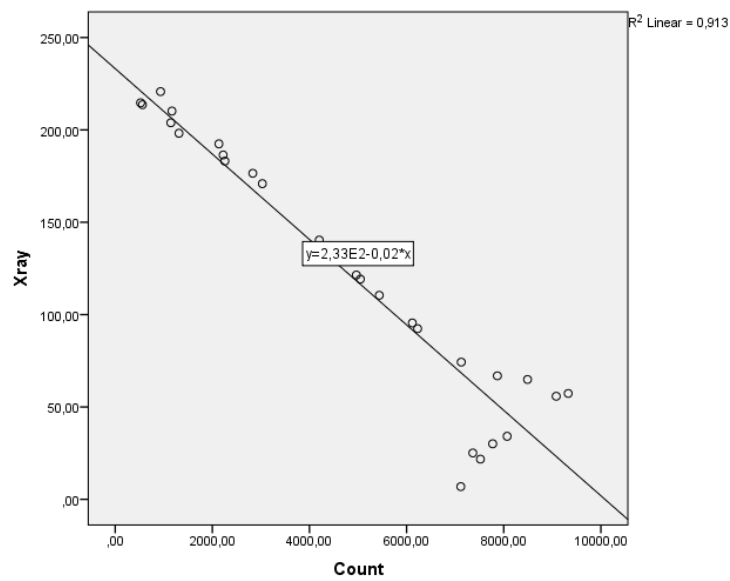


Figure 3.1: Fit graph of the example study 1.

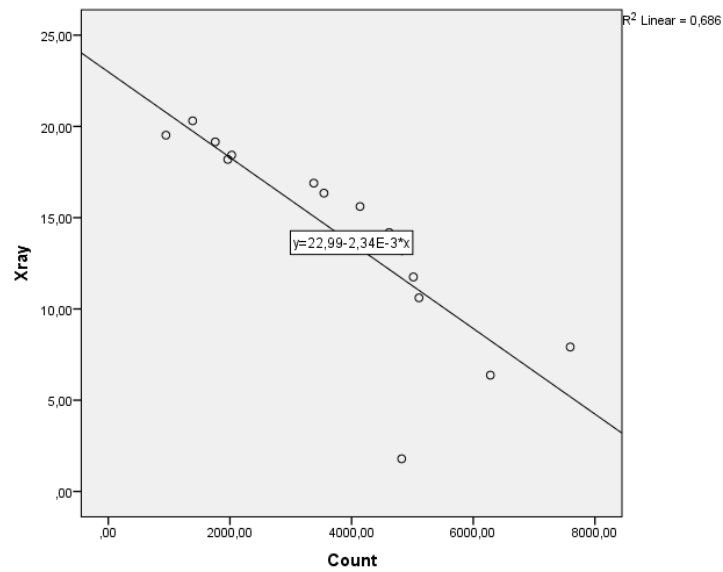


Figure 3.2: Fit graph of the example study 3.

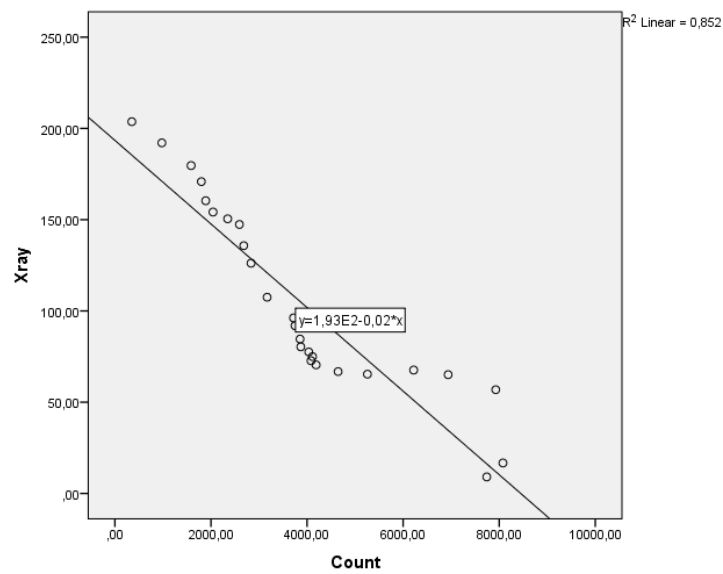


Figure 3.3: Fit graph of the example study 4.

The example curve fitting graphs results for the models are given in Figures 3.4 and 3.5. These graphs demonstrate how much the curve approximates the given data points.

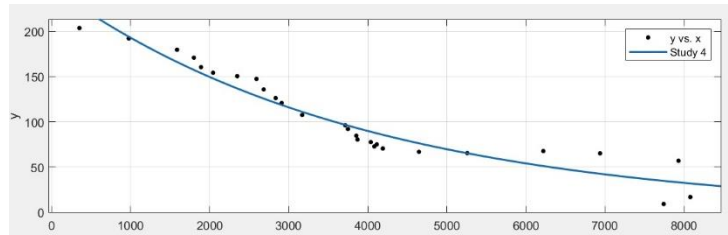


Figure 3.4: Exponential Curve Fitting for Study 4.

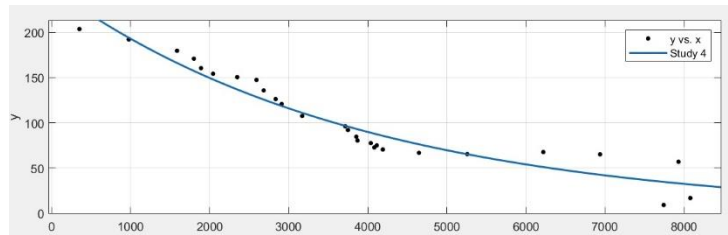


Figure 3.5: Polynomial curve fitting for study 2.

The goodness of fit results for each study is given in Table 3.2, 3.3, 3.4, 3.5 and 3.5. These tables include R^2 and Adjusted R^2 to understand the suitability of the modelled curve to fit an equation to the original data points.

Table 3.2: Goodness of fit results for study 1

Model Name	R^2	Adjusted R^2
Custom Equation	-	-
Exponential	0.1	0.7
Fourier	0.3	0.2
Gaussian	-	-
Linear Fitting	0.1	0.1
Polynomial	0.1	0.1
Power	0	0
Rational	-2.3	0
Smoothing Spline	0.9	0.6
Sum of Sine	0.1	0
Weibul	-3.5	-3.7

The Custom Equation model and the Gaussian could not be applied for Study 1.

Table 3.3: Goodness of fit results for study 2

Model Name	R^2	Adjusted R^2
Custom Equation	$2.2e^{-16}$	-0.7
Exponential	0.9	0.9
Fourier	0.9	0.9
Gaussian	0.9	0.9
Linear Fitting	0.8	0.8
Polynomial	0.9	0.9
Power	0.7	0.7
Rational	0.8	0.8
Smoothing Spline	0.9	0.9
Sum of Sine	0.9	0.9
Weibul	-3.2	-3.4

Table 3.4: Goodness of fit results for study 3

Model Name	R^2	Adjusted R^2
Custom Equation	$4.2e^{-16}$	-0.2
Exponential	0.7	0.7
Fourier	0.7	0.7
Gaussian	0.7	0.7
Linear Fitting	0.6	0.6
Polynomial	0.7	0.7
Power	0.6	0.5
Rational	-5.6	-6.1
Smoothing Spline	0.8	-0.8
Sum of Sine	0.7	0.6
Weibul	-7.2	-7.8

Table 3.5: Goodness of fit results for study 4

Model Name	R^2	Adjusted R^2
Custom Equation	0	-0.1
Exponential	0.9	0.9
Fourier	0.9	0.9
Gaussian	0.9	0.9
Linear Fitting	0.7	0.6
Polynomial	0.9	0.8
Power	0.7	0.7
Rational	-3.0	-3.2
Smoothing Spline	1	1
Sum of Sine	0.9	0.8
Weibul	-4.4	-4.6

Table 3.6: Goodness of fit results for study 5

Model Name	R^2	Adjusted R^2
Custom Equation	$1.1e^{-16}$	-0.2
Exponential	0	0
Fourier	0.2	0
Gaussian	-0.5	-0.7
Linear Fitting	0.1	0.1
Polynomial	0.1	0.1
Power	0	0
Rational	0	0
Smoothing Spline	1	0.8
Sum of Sine	0.1	-0.1
Weibul	-2.1	-2.3

In Table 3.7, the general equation for the models and the equations of each model for each study is given. These equations give the coefficients for the best curve fits of the model.

Table 3.7: Curve fitting equations for studies

Model Name	General Equation	Coefficients of Study 1	Coefficients of Study 2	Coefficients of Study 3	Coefficients of Study 4	Coefficients of Study 5
Custom Equation	$f(x)=a.exp(-bx) +c$		$a=0.09, b=0.21, c=123$	$a=0.551, b=0.579, c=14.02$	$a=0.188, b=0.738, c=105.4$	$a=-35.57, b=18.3, c=32.35$
Exponential	$f(x)= a.exp(bx)$	$a=84.57, b=0.006$	$a=262, b=-0.0002$	$a= 25.35, b=-0.0002$	$a=248.9, b=-0.0003$	$a=34.59, b=-0.0013$
Fourier	$f(x)= a0 + a1.cos(xw) +b1.sin(xw)$	$a0=136.5, a1=16.06, b1=-68.35, w=0.07$	$a0=126.5, a1=77.63, b1=27.71, w=0.0004$	$a0=13.11, a1=2.874, b1=5.811, w=0.0006$	$a0=189.5, a1=39.76, b1=-148.8, w=0.0002$	$a0=37.02, a1=-23.37, b1= 14.65, w=0.1513$
Gaussian	$f(x)=a1.exp(-(x-b1)/c1)^2)$		$a1=217.7, b=-225.2, c1= 6538$	$a1=20.73, b=-43.78, c1=6340$	$a1= 953.5, b1=-1.325e+04, c1=1.22e+04$	$a1=66.53, b1=17.52, c1=14.86$
Linear Fitting	$f(x)= a(\sin(x-\pi)) + b*((x-10)^2) +c$	$a=3.72, b=0.009, c=91.27$	$a=-4.571, b=-2.309e-06, c=192.6$	$a=92.21, b=-2.681e-07, c=18.42$	$a=0.285, b=-2.206e-06, c=146.8$	$a=10.82, b=-0.0002, c=27.59$
Polynomial	$f(x) = p1x +p2$	$p1=0.624, p2=83.72$	$p1=-0.023, p2=233.4$	$p1=-0.002, p2=22.99$	$p1=-0.0228, p2=193$	$p1=-0.044, p2=34.68$
Power	ax^b	$a=75.76, b=0.093$	$a=3865, b=-0.4274$	$a=426.9, b=-0.425$	$a=3015, b=-0.419$	$a=34.9, b=-0.025$
Rational	$f(x)=(p1)/(x+q1)$	$p1=1.25e+08, q1=1.26e +0.6$	$p1=7.97e+05, q1=2737$	$p1=2228, q1=-1292$	$p1=4.48e+04, q1=-803.5$	$p1=2.54e+04, q1=738.4$
Smoothing Spline	$f(x)=\text{piecewise polynomial}$	$p=0.998$	$p=1.01e-05$	$p=9.002$	$p=7.67e-06$	$p=0.97$
Sum of Sine	$f(x)=a1\sin(b1x+c1)$	$a1=1246, b1=0.0005, c1=0.067$	$a=1810, b1=1.274e-05, c=3.013$	$a1=159.1, b1=1.471e-05, c1=2.997$	$a1=3141, b1=7.192e-06, c1=3.081$	$a1=41.23, b1=0.011, c1=0.82$
Weibul	$f(x)=abx^b(b-1)\exp(-ax^b)$	$a=0.018, b=1.727$	$a=0.5772, b=0.2214$	$a=0.9643, b=0.1238$	$a=0.7886, b=0.3002$	$a=0.0217, b=2.394$

3.2 Discussion

In this study, one of the parameters for pyroelectric x-ray generation was investigated. Data for count number and x-ray energy was obtained from four studies. These four studies include five graphs that show x-ray energy and the count number of crystals. Data consist of a minimum of thirty data points; these points are used to create a linear regression model for each study. Table 3.1 shows regression model parameters obtained from SPSS. The values show us Study 2 and Study 5 cannot be used to create an efficient model with linear regression since their p-value is under 0.05. Equations from these two studies are not well-fitted equations since they are not statistically meaningful. The reason for not establishing an efficient model from these studies originated from the count numbers of the studies. As mentioned before, graphs of Study 2 and Study 5 have a count range between 0-200, while others have 0-10⁵.

Equations 3.1, 3.3 and 3.4 are well-fitted linear equations. These equations are suitable to use in simulation studies of pyroelectric x-ray generators and radiography devices. R values for the Studies 1, 3 and 5; 0.91, 0.69 and 0.85 respectively. Since R values are in the range of [-1,1] and higher values mean better fit, these three models are considered as highly fitted to their crystals' characteristics. The graphs from Figures 3.1, 3.2 and 3.3 show the visual representation of the linear regression equation for the models. From these graphs how much, the linear regression approximated the real data points can be understood. For these examples, meaningful results were selected. Although these are the best fits for the linear regression results; to obtain better results the curve fitting methods are needed.

Results from the curve fitting toolbox of MATLAB gives at least one appropriate model type for every study. The Smoothing Spline model gave the best results for every study data. R² values are 0.9, 0.9, 0.8, 0.9 and 1 for Study 1, Study 2, Study 3, Study 4 and Study 5 respectively. Like R values, R² values are also in the range of [-1,1] and again higher values imply a better fit. Study 1, Study 3 and Study 5 are only suitable to be modelled by Smoothing of Spline since the R² values of them for other models are either too low or not in the range. Study 2 and Study 4 can be modelled

with more curve-fitting options since they have an R^2 value of 0.9 for Exponential, Gaussian, Polynomial and Sum of Sine methods. Also, Study 4 has a better fit with Smoothing of Spline; its R^2 value is 1. The negative R^2 results mean the insignificance of explanatory variables. This issue may be overcome by increasing the number of data points used for the evaluation of the model. Figure 3.4 and 3.5 demonstrates the curve fittings for selected studies and models. When these graphs are compared with the graphs of linear regression models, the better fits of the curve fitting methods can be seen. These results signify that the relationship between the X-ray energy and the count number of the crystal can be described by a curve rather than a linear line.

Even though the studies for pyroelectric x-ray generation increase, there is no study about the effect of count number on x-ray energy yield. Thus, this study develops a new perspective to understand pyroelectric x-ray generation. The main goal of this thesis was to be a step closer to a radiography device that uses pyroelectric crystals. Nevertheless, due to a lack of financial support, material supply and creating an experimental environment was interrupted. Still, this study provided new findings to the research field with model results that highly fit actual material.

Chapter 4

Conclusion

Effect of count number of the crystal on x-ray energy investigated in this study. The linear regression analysis was used to investigate the relationship. Curve fitting methods results were well enough to use in further studies for the models. The relationship between count number and x-ray energy has an impact on understanding the pyroelectrical x-ray generation process. The pyroelectrical x-ray generation may start a new era for radiography devices. Since pyroelectrical x-ray generation uses less energy than the traditional method, it may decrease the energy costs of devices. The dimensions of x-ray generators with pyroelectric crystals are smaller than the regular x-ray tubes so smaller device designs become possible with these generators. Specifically, for dental imaging devices, smaller and lightweight device designs may increase the efficiency of dental radiography devices. Radiography methods are widely used in dentistry for diagnosis and treatment purposes. Despite the new modalities, x-ray-based imaging still has a wide range of applications. By the pyroelectric x-ray generator usage in x-ray-based imaging devices, some of the limitations in this field may resolve and effective devices for healthcare may be developed.

References

- [1] Malone J. X-rays for medical imaging: Radiation protection, governance and ethics over 125 years. *Physica Medica* 2020; 79: 47-64. doi.org/10.1016/j.ejmp.2020.09.012
- [2] Haidekker MA. *Medical Imaging Technology*, 1st ed. Springer-Verlag New York; 2013.
- [3] Shah N, Bansal N, Logani A. Recent advances in imaging Technologies in dentistry. *World Journal of Radiology* 2014; 6(10): 794-807. doi.org/10.4329/wjr.v6.i10.794
- [4] Cember H, Johnson TE. *Introduction to Health Physics*, 4th ed. McGraw-Hill; 2008.
- [5] Lisle DA. *Imaging for Students*, 4th ed. Hodder Arnold; 2012.
- [6] International Atomic Energy Agency. Training Material. [Online] [Access date 01.2021]
- [7] Mikla VI, Mikla VV. *Medical Imaging Technology*, 1st ed. Elsevier; 2014.
- [8] Nett, B. Animated CT Generations (1st, 2nd, 3rd, 4th, 5th Gen CT) for Radiologic Technologists [Online]. [Access date: 01.2021] <https://howradiologyworks.com/ctgenerations/>
- [9] Bronzino JD. *The Biomedical Engineering Handbook Medical Device and Systems*, 3rd ed. CRC Press; 2006.

- [10] Idress M. An Overview on MRI Physics and Its Clinical Applications. International Journal of Current Pharmaceutical & Clinical Research 2014; 4: 185-193.
- [11] Zhang X, Smith N, Webb A. Biomedical Information Technology, 2nd ed. Academic Press; 2020.
- [12] Sueten P. Fundamentals of Medical Imaging, 2nd ed. Cambridge University Press; 2009.
- [13] Dougherty G. Digital Image Processing for Medical Applications, 1st ed. Cambridge University Press; 2009.
- [14] Carroll QB. Radiography in the digital age: Physics, exposure, radiation biology, 15th ed. Springfield; 2011.
- [15] International Atomic Energy Agency. Diagnostic Radiology Physics, 1st ed. IAEA; 2014.
- [16] Flower MA. Webb's Physics of Medical Imaging, 2nd ed. CRC Press; 2012.
- [17] Iniewski K. (Ed.) Medical Imaging: Principles, Detectors, and Electronics; 2009.
- [18] Pauwels R. History of Dental Radiography: Evolution of 2D and 3D Imaging Modalities. Medical Physics International Journal 2020; 3: 235-277.
- [19] Iannucci JM, Howerton LJ. Dental Radiography Principles and Techniques, 4th ed. Elsevier; 2011.
- [20] Egeli SS, Isler Y. Mini Review on Dental Imaging Devices and Use of Artificial Intelligence in Dentistry. Journal of Intelligent Systems with Applications 2020; 3(2): 114-117.
- [21] Marotti J, Heger S, Tinschert J, Tortamano P, Chuembou F, Radermacher K. et al. Recent advances of ultrasound imaging in dentistry- a review of the literature. Oral surgery, oral medicine, oral pathology and oral radiology 2013; 115(6): 819-832. doi.org/10.1016/j.oooo.2013.03.012

- [22] Cember H. Introduction to Health Physics, 4th ed. McGraw-Hill Professional Publishing; 2000.
- [23] Frankel RI. Centennial of Rontgen's discovery of x-rays. West J Med 1996; 164(6):497-501.
- [24] International Atomic Energy Agency. Radiation Protection in Digital Radiology, Training Material. [Online]. [Access date: 02.2021]. <https://www.iaea.org/resources/rpop/resources/training-material#1>
- [25] Hendee WR, Ritenour ER. Medical Imaging Physics, 4th ed. Wiley-Liss, Inc; 2002.
- [26] Nascimento M. Brief history of X-ray tube patents. World Patent Information 2014;37: 48-53. doi.org/10.1016/j.wpi.2014.02.008
- [27] Kiuntke F. Making competitors into partners. [Online]. [Access date: 02.2021]. https://www.siemens.com/history/en/news/1065_x-raytube.htm
- [28] Behling R, Grüner F. Diagnostic X-ray sources—present and future. Nuclear Instruments and Methods in Physics Research Section A: Accelerators, Spectrometers, Detectors and Associated Equipment 2018;878: 50-57.
- [29] Parmee RJ, Collins CM, Milne WI, Cole MT. X-ray generation using carbon nanotubes. Nano Convergence 2015; 2(1). doi.org/10.1186/s40580-014-0034-2
- [30] Behling R. Modern Diagnostic X-Ray Sources: Technology, Manufacturing, Reliability, 1st ed. CRC Press; 2015.
- [31] Amptek. COOL-X X-Ray Generator. [Online] [Access date: 02.2021]
- [32] Isler Y, Egeli SS, Manalp A. New-Age Pyroelectric Radiographic X-Ray Generators. Natural and Engineering Sciences 2019; 4(2): 125-132. doi.org/10.28978/nesciences.567072
- [33] Lang S. Pyroelectricity: From Ancient Curiosity to Modern Imaging Tool. Physics Today 2005; 58(8): 31-36. doi.org/10.1063/1.2062916

- [34] Whatmore RW. Pyroelectric Devices and Materials. Reports on Progress in Physics 199; 49(12). doi.org/10.1088/0034-4885/49/12/002
- [35] Nasser M. A virtual experiment on pyroelectric X-ray generator. Nuclear Instruments and Methods in Physics Research Section B: Beam Interactions with Materials and Atoms 2015; 358: 255-257. doi.org/10.1016/j.nimb.2015.06.035
- [36] Safari A, Jadidian B, Akdogan EK. Piezoelectric Composites for Transducer Applications. Comprehensive Composite Materials 2000; 5:533-561. doi.org/10.1016/B0-08-042993-9/00095-4
- [37] Danon Y. A Novel Compact Pyroelectric X-Ray and Neutron Source. United States, 2007.
- [38] Lang S.B. Sourcebook of Pyroelectricity, 1st ed. Gordon and Breach Science Publishers; 1974.
- [39] Zhao XG, Chu JH, Tang Z. Magnetic Properties Heisenberg Exchange Interaction and Curie Temperature of CdS Nanoclusters. Journal of Physical Chemistry 2015; 119(52) :29071-29075.
- [40] Sakayori KI, Matsui Y, Abe H. Curie Temperature of BaTiO₃. Japanese Journal of Applied Physics 1995;34(1): 5443-5445.
- [41] Rosenblum B, Braunlich P, Carrico JP. Thermally stimulated field emission from pyroelectric LiNbO₃. Applied Physics Letters 1974; 25: 17-19. doi.org/10.1063/1.1655260
- [42] Brownridge JD, Shafroth SM. Electron Beam Production by Pyroelectric Crystals. Physics 2002.
- [43] Geuther J, Danon Y. Electron and positive ion acceleration with pyroelectric crystals. Journal of Applied Physics 2005; 97. doi.org/10.1063/1.1884252
- [44] Brownridge JD, Pyroelectric X-ray generator. Nature 1992; 358: 287-288. doi.org/10.1038/358287b0

- [45] Hanamoto K, Kataoka T, Yamaoka K. Pressure dependence of X-rays produced by an LiTaO₃ single crystal over a wide range of pressure. *Applied Radiation and Isotopes* 2018;1 35: 40-42. doi.org/10.1016/j.apradiso.2018.01.019
- [46] Geuther J, Danon Y, Saglime F, Sones B. Electron acceleration for X-ray production using paired pyroelectric crystals. *Sixth International Meeting on Nuclear Applications of Accelerator Technology: Accelerator Applications in a Nuclear Renaissance*; 2003 Jun 1-3; San Diego CA, United States. 2003. 591-595.
- [47] Hanamoto K, Kawabe A, Sakoda A, Kataoka T, Okada M, Yamaoka K. Pressure dependence of X-rays produced by an LiTaO₃ single crystal at low pressures. *Nuclear Instruments and Methods in Physics Research Section A: Accelerators, Spectrometers, Detectors and Associated Equipment* 2012; 669: 66-69. doi.org/10.1016/j.nima.2011.12.028
- [48] Brownridge JD, Shafroth SM. X-ray fluoresced high-Z (up to Z = 82) K-x-rays produced by LiNbO₃ and LiTaO₃ pyroelectric crystal electron accelerators. *Applied Physics Letters* 2004; 85(7): 1298-1300. doi.org/10.1063/1.1782260
- [49] Karadede, Y. A hybrid algorithm approach to curve fitting problems (master's thesis). Isparta: Suleyman Demirel University; 2014.
- [50] Islam T. Learning SPSS without Pain: A Comprehensive Manual for Data Analysis and Interpretation of Outputs, 1st ed. 2020. doi.org/10.6084/m9.figshare.12812837.v1
- [51] Greenland S, Senn SJ, Rothman KJ, Carlin JB, Poole C, Goodman SN, et al. Statistical tests, P values, confidence intervals, and power: a guide to misinterpretations. *European Journal of Epidemiology* 2016; 31(4): 337-350. doi.org/10.1007/s10654-016-0149-3
- [52] Thiese MS, Ronna B, Ott U. P value interpretations and considerations. *Journal of Thoracic Disease* 2016; 8(9): 928-931. doi.org/10.21037/jtd.2016.08.16

- [53] Profillidis VA, Botzoris GN. Statistical Methods for Transport Demand Modelling, Elsevier; 2019.
- [54] Vidyullatha P, Rajeswara RD. Machine Learning Techniques on Multidimensional Curve Fitting Data Based on R-Square and Chi-Square Methods. International Journal of Electrical and Computer Engineering (IJECE) 2015; 6: 974-979. doi.org/10.11591/ijece.v6i3.9155
- [55] Akossou AYJ, Palm R. Impact of Data Structure on the Estimators R-Square and Adjusted R-Square in Linear Regression. International Journal of Mathematics and Computation 2013; 20 (3).
- [56] Kumari K, Yadav S. Linear regression analysis study. Journal of the Practice of Cardiovascular Sciences 2018; 4(1): 33-36. doi.org/10.4103/jpcs.jpcs_8_18
- [57] Mathworks. Curve Fitting Toolbox User's Guide. Version 1. [Online] [access date: 9.2021] <https://www.mathworks.com/>
- [58] Landau S, Everitt B. A handbook of statistical analyses using SPSS, 15th Ed. Boca Raton: Chapman & Hall/CRC; 2003.
- [59] Hilbe J. A review of current SPSS products: SPSS 12, SigmaPlot 8.02, SigmaStat 3.0, Part 1. The American Statistician 2003; 57; 310-315. doi.org/10.1198/0003130032495
- [60] Mathworks. Getting Started with MATLAB. Version 7. [Online] [access date: 5.2021] <https://www.mathworks.com/>

Appendices

Appendix A

Publications from the Thesis

Journal Articles

1. S.S. Egeli, Y. Isler, Piroelektrik Malzemelerde Döngü Sayısı ile X Işını Enerji Seviyesi Arasındaki İlişkinin Doğrusal Regresyon Analizi ile Belirlenmesi (Determining the Relation Between the Count Number and X-Ray Energy Level in Pyroelectric Materials using Linear Regression Analysis), Journal of Intelligent Systems with Applications, 4(1): 58-60, 2021.
2. S.S. Egeli, and Y. Isler, Dental Görüntüleme Cihazları ve Diş Hekimliğinde Yapay Zekanın Kullanımı Üzerine Kısa İnceleme (Mini Review on Dental Imaging Devices and Use of Artificial Intelligence in Dentistry), Journal of Intelligent Systems with Applications, 3(2): 114-117, 2020.
3. Y. Isler, S.S. Egeli, and A. Manalp, Investigating New-Age Pyroelectric Radiographic X-Ray Generators, (Review), Natural and Engineering Sciences, 4(2): 125-132, 2019.

Curriculum Vitae

Name Surname : Saadet Sena Egeli

EDUCATION

Master of Science / Department of Biomedical Engineering 2019- 2021

The Graduate School of Natural and Applied Sciences

Izmir Katip Celebi University (Dissertation Stage, GPA:4.0)

*Thesis: Design of Pyroelectrical Crystal Based X-Ray Generator for
Dentistry Applications*

Bachelor's degree / Department of Biomedical Engineering 2015- 2019

Faculty of Engineering and Architecture

Izmir Katip Celebi University (GPA: 3.04)

Thesis: Investigation of Pyroelectric Crystal Based X-Ray Generators

PROFESSIONAL EXPERIENCE

Quality Control Specialist 09.2021- Current

Chil Medical Devices

Research and Development Engineer

Islerya Medical and Information Technologies 02.2020- 07.2021

PUBLICATIONS

1. Y. Isler, S. S. Egeli, and A. Manalp, "Investigating New-Age Pyroelectric Radiographic X-Ray Generators," Natural and Engineering Sciences, vol. 4, no. 2, pp. 125-132, 2019.
2. S.S. Egeli, and Y. Isler, Development of Artificial Intelligence Algorithm for Early Diagnosis of Sepsis Disease, 3rd International Conference on Medical Devices (TIPCIH'2020), Adrasan - Antalya / Turkey, 28-29 September 2020.

3. M.B. Selek, S.S. Egeli, and Y. Isler, Patient Survival Prediction with Machine Learning Algorithms, ICAII4.0 - International Conference on Artificial Intelligence towards Industry 4.0, Izmir / Turkey, 12-14 November 2020.
4. S.S. Egeli, and Y. Isler, Mini Review on Dental Imaging Devices and Use of Artificial Intelligence in Dentistry, ICAII4.0 - International Conference on Artificial Intelligence towards Industry 4.0, Izmir / Turkey, 12-14 November 2020.
5. M.B. Selek, B. Yesilkaya, S.S. Egeli, and Y. Isler, Investigating Orange Software as a Pattern Recognition Visual Programming Tool, 3rd International Conference of Applied Sciences, Engineering and Mathematics (IBU-ICASEM 2021), June 3-5, Skopje/North Macedonia, 2021.
6. M.B. Selek, B. Yesilkaya, S.S. Egeli, Y. Isler, The effect of principal component analysis in the diagnosis of congestive heart failure via heart rate variability analysis, Proceedings of the Institution of Mechanical Engineers, Part H: Journal of Engineering in Medicine, 2021.
7. Y. Isler, A. Manalp, and S.S. Egeli, Tüketici Elektroniği Bileşenleri Kullanarak Alternatif Bir Raspberry Pi Tabanlı X-Işını Görüntüleme Cihazı Tasarımı (An Alternative Design of X-Ray Imaging Device based on Raspberry Pi with Consumer Electronic Components), Karaelmas Fen ve Mühendislik Dergisi (Karaelmas Science and Engineering Journal), ACCEPTED, 2021.
8. S.S. Egeli, Y. Isler, Piroelektrik Malzemelerde Döngü Sayısı ile X Işını Enerji Seviyesi Arasındaki İlişkinin Doğrusal Regresyon Analizi ile Belirlenmesi (Determining the Relation Between the Count Number and X-Ray Energy Level in Pyroelectric Materials using Linear Regression Analysis), Journal of Intelligent Systems with Applications, 4(1): 58-60, 2021.
9. B. Yesilkaya, S.S. Egeli, Y. Isler, Diagnosis of Ovarian Cancer using Conventional Machine Learning Methods, ICAII4.0 - International Conference on Artificial Intelligence towards Industry 4.0, Iskenderun / Turkey, 11-12 November 2021, ACCEPTED.

PROFESSIONAL SKILLS

C Programming, Python Programming, MATLAB Programming, FPGA Programming with VHDL, Arduino, Hobby Electronics SolidWorks, Statistical Package for the Social Sciences (SPSS), Microsoft Office: Microsoft Word, Excel, PowerPoint, Outlook, OneNote, LaTeX: Professional writing

CERTIFICATIONS

ISO 13485:2016 Medical Devices Quality Management Systems Basic Training	2021
ISO 9001:2015 Quality Management Systems Basic Training	2021
Foundations of Healthcare Systems Engineering	2020
Project Management Training (TOBB University of Economics and Technology)	2020
Machine Learning and Python	2020
Clinical Engineering Training Services in Turkey	2016
XX. Biomedical Engineering National Meeting	2016
Comenius Project Green Buildings- Italy and Turkey	2014

AWARDS

Design of Pyroelectric Crystal Based Dental Radiography Device, **Accepted to the Final Stage** of TUBITAK 2242 Projects Fair in İzmir Region